frontiers

Stable isotope tracing reveals compartmentalized nitrogen assimilation in scleractinian corals

Eric N. Chiles[1, 2], Ariana S. Huffmyer[3, 4], Crawford Drury[5], Hollie M. Putnam[3], Debashish Bhattacharya[6], Xiaoyang Su[2, 7*]

[1]School of Graduate Studies, Rutgers University, United States, [2]Rutgers Cancer Institute of New Jersey, Rutgers, The State University of New Jersey, United States, [3]Department of Biological Sciences, University of Rhode Island, United States, [4]School of Aquatic and Fishery Sciences, College of the Environment, University of Washington, United States, [5]Hawaii Institute of Marine Biology, University of Hawaii at Manoa, United States, [6]Department of Biochemistry and Microbiology, School of Environmental and Biological Sciences, Rutgers, The State University of New Jersey, United States, [7]Department of Medicine, Robert Wood Johnson Medical School, Rutgers, The State University of New Jersey, United States

Submitted to Journal:
Frontiers in Marine Science

Specialty Section:
Coral Reef Research

Article type:
Original Research Article

Manuscript ID:
1035523

Received on:
02 Sep 2022

Revised on:
24 Oct 2022

Journal website link:
www.frontiersin.org

Conflict of interest statement

The authors declare that the research was conducted in the absence of any commercial or financial relationships that could be construed as a potential conflict of interest

Author contribution statement

ENC, XS, and DB conceived the study. ENC and XS designed the fieldwork experiment strategy. HMP provided coral tissues for analysis, ENC, AH, HMP, and CD performed the fieldwork experiments. ENC analyzed the samples and performed the bioinformatics. ENC, XS, DB, and AH contributed to data interpretation. ENC wrote the original draft of the manuscript. XS, DB, HMP, AH, and CD revised the original draft. All authors have read and approve of the submitted version of the manuscript.

Keywords

nitrogen assimilation, stable isotope, holobiont, compartmentalization, LCMS, Metabolomics

Abstract

Word count: 249

Corals form symbiotic relationships with dinoflagellate algae of the family Symbiodiniaceae, bacteria, and other microbes. Central to that relationship is the regulation of nutrition flux between the animal host and the photosynthetic Symbiodiniaceae that it is reliant on for the majority of metabolic needs. Nitrogen availability controls the growth and density of Symbiodiniaceae within coral tissues and has been proposed to play a role in host derived symbiosis regulation. Warming ocean temperatures and subsequent increases in dissolved organic carbon can potentially increase nitrogen fixation and lead to bleaching. We investigated the importance of nitrogen metabolism in vivo with LC-MS based stable isotope tracing using nubbins from three species of Hawaiian coral, the more heat tolerant Montipora capitata and Porites compressa and the more heat sensitive Pocillopora acuta, that were collected from reefs in Kāneʻohe Bay, Oʻahu. In addition to 15N incorporation into nucleotides, amino acids, and urea cycle metabolites, we also observed significant isotopic labeling in dipeptides, supporting their previous identification as major heat stress response metabolites. Surprisingly, the dipeptides are highly enriched in 15N compared to free amino acids, which are the biosynthetic precursors for dipeptides. This suggests that there is a high turnover of dipeptide pools and distinct biosynthetic mechanisms that separately mediate amino acid and dipeptide production. These preliminary data show that nitrogen assimilation in the coral holobiont is likely compartmentalized, with rapid assimilation and quick dipeptide turnover occurring in one region of the holobiont and slow turnover of other nitrogen containing metabolites in other region(s).

Contribution to the field

Worldwide, coral reefs are facing mass mortality events and potential extinction due to anthropomorphic climate change. As global ocean temperatures continue to rise beyond the thermal maxima of corals, the metabolic balance of these animals is threatened by bleaching and subsequent nutrient starvation. This will undoubtedly have profound consequences for the biodiverse aquatic ecosystems they support and nations that are dependent on the reefs as a food source, economic boom, and protective barrier. This has created a need to mechanistically understand how homeostatic metabolism is altered during stress in corals to preserve them. Here, liquid chromatography coupled with mass spectrometry (LCMS) and 15N-ammonia stable isotope tracing is utilized to track nutrient assimilation within the coral holobiont. Our analysis shows nitrogen is incorporated into several metabolite classes such as amino acids, urea cycle metabolites, and dipeptides, a secondary metabolite class previously shown to be significantly enriched during heat stress. We also compare the enrichment of dipeptides and their constitutive amino acids and show there is minimal correlation, leading us to postulate that there are distinct metabolite pools that are compartmentalized to the coral host and the symbiotic algae.

Funding statement

The metabolomics analysis was performed at the Rutgers Cancer Institute of New Jersey Metabolomics Shared Resource and supported, in part, by funding from NCI-CCSG, P30CA072720-5923. This work was supported by a grant from the Catalyst Science Fund-Revive and Restore award to DB and XS, in addition to National Science Foundation award 1756623 to HMP. DB was also supported by NSF grant NSF-OCE 1756616 and a NIFA-USDA Hatch grant (NJ01180).

Ethics statements

Studies involving animal subjects
Generated Statement: No animal studies are presented in this manuscript.

Studies involving human subjects
Generated Statement: No human studies are presented in this manuscript.

Inclusion of identifiable human data
Generated Statement: No potentially identifiable human images or data is presented in this study.

Data availability statement

Generated Statement: The datasets presented in this study can be found in online repositories. The names of the repository/repositories and accession number(s) can be found in the article/supplementary material.

Stable isotope tracing reveals compartmentalized nitrogen assimilation in scleractinian corals

Eric N. Chiles[1,2], Ariana S. Huffmyer[3,4], Crawford Drury[5], Hollie M. Putnam[3], Debashish Bhattacharya[6], Xiaoyang Su[2,7*]

[1]Microbial Biology Graduate Program, Rutgers University, New Brunswick, NJ 08901, USA

[2]Metabolomics Shared Resource, Rutgers Cancer Institute of New Jersey, Rutgers University, New Brunswick, NJ 08901, USA

[3]Department of Biological Sciences, University of Rhode Island, Kingston, RI 02881, USA

[4]School of Aquatic and Fisheries Science, University of Washington, Seattle, WA 98195, USA

[5]Hawai‘i Institute of Marine Biology, University of Hawai‘i at Mānoa, Kāne‘ohe, HI 96744, USA

[6]Department of Biochemistry and Microbiology, Rutgers University, New Brunswick, NJ 08901, USA

[7]Department of Medicine, Division of Endocrinology, Robert Wood Johnson Medical School, Rutgers University, New Brunswick, NJ 08901, USA

*** Correspondence:**
Xiaoyang Su
xs137@rwjms.rutgers.edu

Keywords: nitrogen assimilation, stable isotope, holobiont, compartmentalization, LCMS, metabolomics.

Abstract

Corals form symbiotic relationships with dinoflagellate algae of the family Symbiodiniaceae, bacteria, and other microbes. Central to that relationship is the regulation of nutrition flux between the animal host and the photosynthetic Symbiodiniaceae that it is reliant on for the majority of metabolic needs. Nitrogen availability controls the growth and density of Symbiodiniaceae within coral tissues and has been proposed to play a role in host derived symbiosis regulation. Warming ocean temperatures and subsequent increases in dissolved organic carbon can potentially increase nitrogen fixation and lead to bleaching. We investigated the importance of nitrogen metabolism *in vivo* with LC-MS based stable isotope tracing using nubbins from three species of Hawaiian coral, the more heat tolerant *Montipora capitata* and *Porites compressa* and the more heat sensitive *Pocillopora acuta*, that were collected from reefs in Kāne‘ohe Bay, O‘ahu. In addition to ^{15}N incorporation into nucleotides, amino acids, and urea cycle metabolites, we also observed significant isotopic labeling in dipeptides, supporting their previous identification as major heat stress response metabolites. Surprisingly, the dipeptides are highly enriched in ^{15}N compared to free amino acids, which are the biosynthetic precursors for dipeptides. This suggests that there is a high turnover of dipeptide pools and distinct biosynthetic mechanisms that separately mediate amino acid and dipeptide production. These preliminary data show that nitrogen assimilation in the coral holobiont is likely compartmentalized, with rapid assimilation and quick dipeptide turnover occurring in one region of the holobiont and slow turnover of other nitrogen containing metabolites in other region(s).

1 Introduction

Biogeochemical cycling, the movement of small metabolic intermediates and products between organisms and the larger environment undergirds the ability for complex lifeforms to exist on Earth. This is not limited to terrestrial ecosystems, but extends to the oceans, characterizing the relationship of Scleractinian (reef-building) corals and their photosynthetic dinoflagellate algal endosymbionts, in the family Symbiodiniaceae. Reef building corals are the backbones of biodiverse marine ecosystems (Bourne et al 2016; Cunning and Baker 2013; Tivey et al 2020). Covering < 0.1% of the ocean floor, they house upwards of 25% of all aquatic life (Hoegh-Guldberg et al 2019). This immense diversity is possible via maintenance of the metabolic balance between the scleractinian animal, the Symbiodiniaceae algae, and other microbes that collectively comprise a community referred to as the coral holobiont. The algal symbionts provide up to 95% of the energy requirements of the cnidarian host (Falkowski et al 1993). Within the Symbiodiniaceae, photoautotrophic energy is harnessed to assimilate nutrients and produce organic photosynthates, such as glucose, amino acids, glycerol, and other compounds that are translocated to the host to maintain primary metabolism (Burriesci et al 2012; Cleves et al 2020; Li et al 2021). The focus of the metabolic balance and burden between reef building corals and their symbionts has largely been centered on investigating the fate of carbon within the holobiont (Badger and Price 1992; Whitney et al 1995; Whitney and Yellowlees 1995; Furla et al 2000; Furla et al 2005). The devastating effects of external environmental stressors, predominately arising from anthropogenic climate change, disrupts the coral symbiosis, leading to coral bleaching. If persistent, bleaching can eventually result in extensive reef loss (Loya et al 2001; McClanahan 2002; Nielsen et al 2018; Sogin et al 2016). It is not fully clear how bleaching is mechanistically regulated. Considering that the metabolic substrates the symbionts need must first pass through the host tissues, there are several proposed regulatory mechanisms for how the animal host may exert control over the algal population within its tissues (Li et al 2021).

Relative to the study of carbon compound exchange, the movement of nitrogen throughout the holobiont and how nitrogen metabolism is impacted by environmental stress has not been as extensively investigated across a wide range of coral species. Because ammonium (NH_4^+) accounts for 42% of the nitrogen requirement of the holobiont and is the predominant nitrogenous substrate that is passed to the symbionts from the host (Pernice et al 2012), this raises important questions about how nitrogen metabolism may have a potential mechanistic connection to bleaching and be a means of host control of the symbiont population (Pogoreutz et al 2017; Rädecker et al 2015). Nitrogen sources such as NO3-, urea, and dissolved amino acids can be assimilated by both the coral animal (through heterotrophic feeding or ammonium, nitrate, urea, or amino acid transporters), and assimilated by the symbionts (through an analogous suite of transporters) (Benavides et al 2017; Grover et al 2002, 2003, 2006, & 2008; LeJeunesse et al 2018; Muscatine et al 1979). Symbiodiniaceae have the capacity to take-up and/or fix dissolved inorganic nitrogen from surrounding seawater in the form of NH_4^+ at rates 14 to 23 times greater than the host via three key nitrogen assimilating enzymes. Glutamine synthetase (GS) and glutamine oxoglutarate aminotransferase (GOGAT) transaminate glutamate to produce glutamine, whereas glutamate dehydrogenase (GDH) transaminates α-ketoglutarate to produce glutamate (Roberts et al 2001). Transcriptomic analysis of at least one coral species, *Stylophora pistillata*, showed that the expression of these enzymes in the host is down-regulated while it is unchanged in the algae during heat stress as energy burdens shift and amino acid catabolism pathways become more active (Rädecker et al 2020). Metabolomics analysis can thus greatly expand our understanding of the nitrogen based (and other) metabolic interactions within the holobiont, and elucidate how environmental stressors such as rising water temperatures, may alter the homeostasis of reef building corals and their associated symbiont communities. Dipeptides, for example, are metabolites comprised of amino acids, which provide further relevance to investigating nitrogen

metabolism in reef-building corals because all amino acids contain nitrogen molecules. We previously demonstrated the correlation between dipeptide accumulation and thermal stress, showing that dipeptides are significantly accumulated as heat stress is prolonged (Williams et al 2021). To further elucidate nitrogenous exchange, here we used stable isotope tracing with Liquid Chromatography coupled with Mass Spectrometry (LC-MS) to investigate the metabolic fate of NH_4^+ within holobionts of the Hawaiian corals *Montipora capitata*, *Pocillopora acuta*, and *Porites compressa*, which have differing resistances to thermal stress. (Figures 1A-C) (Bahr et al 2015; Mackay et al 2015; Wilkinson 2016; Zamboni et al 2015). Due to experimental limitations this present study will not be a rigorous comparative analysis of nitrogen assimilation under heat stress, but nonetheless shows the robustness of nitrogen incorporation into primary and secondary metabolites in several coral species. The entire dataset, which does include a time course under heat stress, is available in our MassIVE data repository under project number MSV000090231.

2 Materials and methods

2.1 Coral nubbin cultivation

Three different colonies each of *M. capitata*, *P. acuta*, and *P. compressa* were identified and collected from Kāne‘ohe Bay, HI under SAP 2021-41. Colonies were collected in June of 2021 from a depth of 1-2m and were located within a 25m section of the reef. Each colony was fragmented into 5 cm x 5 cm nubbins at the Hawai‘i Institute of Marine Biology, located on Moku o Lo‘e in Kāne‘ohe Bay, Hawai‘i, and the nubbins were attached to labeled plugs using hot glue on the skeletal base. The plugged nubbins were then dispersed across six plastic treatment tanks (5.7 liter; 18cm x 21cm x 21cm”, L x W x H), with three tanks (biological replicates) for the ambient temperature condition and three tanks for the high temperature treatment condition. All three species were co-cultured in each tank with analogous sample sets being collected for additional analyses. In total, there were nine nubbins (three of each species) in each tank. Stands for the plugged nubbins were fashioned out of white egg crate and PVC pipe, and were constructed to sit approximately 10cm from the bottom of the tank so that nubbins were fully submerged. The individual treatment tanks sat inside of larger water bath tanks (284 liter; 51cm x 91cm, L x W) and were connected to a flow through system with the water supply coming directly from Kāne‘ohe Bay. Each individual treatment tank contained a submersible water pump (Hydor Centrifugal Pump 200 gph, Hydor USA Inc., CA, USA). Following nubbin fragmentation, plugging, and disbursement in tanks, they were allowed to acclimate for four days prior to the temperature ramp of the high temperature water bath housing the three individual high temperature tanks. The sample tanks were maintained outside in order to follow a natural diurnal cycle for the duration of the experiment. A shade cloth was used to protect the plugged coral nubbins.

2.2 Experimental design

The temperature of the water bath was maintained using two water heaters (Aqueon 300W Heater, WI, USA, set to 31°C) and monitored by the Apex aquarium controller (Neptune Systems, CA, USA) that powered the heaters on or off based on constant set points. Both ambient and high temperature water baths were monitored with an Onset Computer Corp HOBO Water Temp Pro temperature logger (resolution 0.02°C at 25°C; accuracy ±0.21°C from 0°C to 50°C). The average temperature of the ambient water bath was 27.1°C ± 0.55°C and the average temperature of the high water bath was 31.0°C ± 0.50°C. The average temperature of the ambient tanks was 27.2°C ±0.40°C and the average temperature of the high tanks was 28.3°C ± 0.65°C.

The temperature ramp occurred over 24 hours in the high treatment tanks. Individual treatment tank conditions were monitored for temperature (Traceable Digital Thermometer), pH &

conductivity/salinity (Orion Star A325 Thermoscientific pH/conductivity meter, accuracy ±0.2 mV or ±0.05% of reading, Thermo Fisher Scientific, MA, USA), and light (MQ-510 Apogee underwater quantum meter model, resolution 0 to 4000 µmol $m^{-2}s^{-1}$; range 389 to 692 nm ± 5 nm). Readings were taken twice daily in the morning and late afternoon or early evening. On average there was a 2.7°C temperature differential between the high temperature water bath and the individual high temperature sample tanks. The stable isotope labeling incubations were executed following a modified method outlined by Hillyer et al 2018. After sampling, specimens were added to watertight jars filled with 100 mL of 1 µm filtered seawater (filtered to 20 µm, 10 µm, 5 µm, and 1 µm in series) that was supplemented with 100 µM ^{15}N-NH$_4$Cl (Cambridge Isotope Laboratories, MA, USA). The incubation jars were autoclaved prior to sampling. Labeling incubations lasted for 18 hours and were maintained at experimental temperatures by being sealed and placed alongside the sample tanks within the water baths. Incubation jars were agitated every 4-6 hours. The concentration was chosen to be commensurate with previous studies that utilized nitrogen supplementation in corals (Li et al 2020).

2.3 Coral sampling

In order to study the effect of heat stress on nitrogen assimilation activities, we took three sampling time points (TPs) for ^{15}N incorporation tests in this study. TP1 was taken on June 15th, 2021, TP2 was taken on June 21st, 2021, and TP3 was taken on June 24th, 2021. TP1 corresponds to 24hrs after the high temperature water bath reaching the set-point temperature, TP3 corresponds to the experiment endpoint at 9 days, and TP2 is the midpoint between TP1 and TP3. At each time point, for each treatment, and each tank, 3 technical replicate clippings were taken and incubated together in the same jar, meaning for each species there were 18 clippings per time point. Immediately after clipping, samples were added to prepped jars containing the labeling incubation seawater and then transferred to the water bath. Sampling was started ≈11:00AM so that incubation periods could begin ≈12:00PM. Following isotopic incubation, the clippings were transferred to sterile Whirl-Paks that were immediately submerged in liquid nitrogen and transferred to −80°C to preserve their metabolic integrity until metabolite extraction.

2.4 Metabolite extraction from coral nubbins

Metabolite extraction from each technical replicate was done individually. Metabolites were extracted using a protocol optimized for water soluble polar metabolite analysis on LC-MS. The extraction solvent used was a (v/v/v) solution of 40:40:20 (Methanol:Acetonitrile:Water) + 0.1M Formic Acid. The extraction buffer was stored at -20°C prior to usage and immediately preceding the metabolite extraction 1mL added to a glass 2mL Dounce homogenizers that had chilled on ice. Pieces of the preserved nubbins were then clipped, weighed, and added to the cold extraction solvent in the homogenizer and left to incubate for 5 minutes. The pestle of the homogenizer was then used to homogenize the coral tissue until there was a visible accumulation of coral skeleton at the bottom of the homogenizer and the homogenate was visibly pigmented. An additional 500µL aliquot of cold 40:40:20 + 0.1M Formic Acid extraction buffer was then used to rinse down the sides of the Dounce and pestle. The total 1.5mL volume was then strained through a 100µm cell strainer (VWR International) into 50mL receptacle. There should be a visible amount of skeleton collected in the strainer. The rest of the homogenate was then transferred to a 1.5mL Eppendorf tube and vortexed for 10 seconds and then centrifuged for 10 minutes at 16,000g at 4°C. After centrifugation, there will be a pellet at the canonical bottom of the tube. A final 500µL aliquot of the homogenate was then pipetted to a second clean Eppendorf tube, to which 44µL of 15% (m/v) NH_4HCO_3 was added to neutralize the acid in the buffer. This process generated the final extract that was ready to be loaded to instrument vials for analysis. The extracts were stored at -80°C until processing.

2.5 UHPLC chromatography conditions

Hydrophilic Interaction Liquid Chromatography (HILIC) separation was performed on a Vanquish Horizon UHPLC system (Thermo Fisher Scientific, Waltham, MA) with XBridge BEH Amide column (150 mm × 2.1 mm, 2.5 µm particle size, Waters, Milford, MA) using a gradient of solvent A (95%:5% H_2O:acetonitrile with 20 mM acetic acid, 40 mM ammonium hydroxide, pH 9.4), and solvent B (20%:80% H_2O:acetonitrile with 20 mM acetic acid, 40 mM ammonium hydroxide, pH 9.4). The gradient was 0 min, 100% B; 3 min, 100% B; 3.2 min, 90% B; 6.2 min, 90% B; 6.5 min, 80% B; 10.5 min, 80% B; 10.7 min, 70% B; 13.5 min, 70% B; 13.7 min, 45% B; 16 min, 45% B; 16.5 min, 100% B and 22 min, 100% B. The flow rate was 300 µL/min. Injection volume was 5 µL and column temperature was 25 °C. The autosampler temperature was set to 4°C and the injection volume was 5 µL.

2.6 Full scan mass spectrometry

The full scan mass spectrometry analysis was performed on a Thermo Q Exactive PLUS with a HESI source which was set to a spray voltage of -2.7kV under negative mode and 3.5kV under positive mode. The sheath, auxiliary, and sweep gas flow rates of 40, 10, and 2 (arbitrary unit) respectively. The capillary temperature was set to 300°C and aux gas heater was 360°C. The S-lens RF level was 45. The m/z scan range was set to 72 to 1000m/z under both positive and negative ionization mode. The AGC target was set to 3e6 and the maximum IT was 200ms. The resolution was set to 70,000.

2.7 Data analysis

The metabolite abundance data were obtained from the MS^1 full scans using MAVEN (Melamud et al 2010). Base peaks and labeled fractions were verified with manual peak picking using a mass accuracy window of 5 ppm. The isotope natural abundance were corrected using AccuCor (Su et al 2017). Statistical significance of metabolite enrichment was determined by a Student's t test that assumed unequal variance.

2.8 Calculated enrichment formula

Mathematically, the expected enrichment of a dipeptide can be calculated using the following generalized formula:

$$E_{\text{Dipeptide}} = \frac{E_{AA1} \times n_{AA1} + E_{AA2} \times n_{AA2}}{n_{AA1} + n_{AA2}}$$

In which E_{AA} denotes the enrichment of amino acid AA and n_{AA} denotes the number of nitrogen atoms in amino acid AA.

3 Results

3.1 Heat-stress and light treatments

The goal of this study was two-fold. First, we wished to investigate how ammonium is assimilated to amino acids, nucleotides, urea cycle intermediates, dipeptides, and other nitrogen containing metabolites. Second, we were interested in how heat-stress affects nitrogen assimilation. For the heat-stress treatment, the coral nubbins of each species, from three different colonies were collected and subjected to acute heat stress for 9 days. On day 1 (TP1), day 5 (TP2), and day 9 (TP3) after the temperature ramp up, sample fragments of the nubbins were harvested for stable isotope incubations

lasting 18 hours in filtered seawater taken directly from Kāne'ohe Bay that was supplemented with 100 µM $^{15}NH_4Cl$ (Figure 1D). Stable isotope labeling allowed metabolite production to be traced through a metabolic pathway to determine which metabolites incorporate the isotopic tracer, which provides insights into metabolite biosynthesis mechanisms and pathway flux (Figure 1E) (Jang et al 2018). The samples were subjected to targeted polar metabolite analysis. Because both the symbiont and the host assimilate NH_4^+, that they can subsequently share, we analyzed the holobiont in toto.

The water bath housing the high temperature tanks was heated to 31°C, whereas the control tank was maintained at ambient temperature. Although the water bath heating did maintain the high treatment tanks at an elevated temperature than the ambient treatment, the temperatures directly subjected to the nubbins were lower than anticipated. The daily recorded temperature difference between the ambient and high treatment tanks was within 1-1.5°C of each other (Figure 1F). In addition, the temperature of the high treatment tanks did not consistently reach above 29°C, which is within the local thermal range of the coral nubbins. Collectively, this resulted in a heat stress that was less significant than intended.

Unexpectedly, the high temperature tanks received lower light compared to the ambient temperature tanks (Figure 1G). As a result, changes to the metabolome observed over the duration of the experiment can be attributed to either the temperature or the light difference. Light is an energy source for the photosynthetic Symbiodiniaceae, therefore, light deprivation impacts the cnidarian host by potentially creating a nutrient limited state that may arrest growth (Forsman et al 2012). This is tantamount to a compounding stress condition extraneous to our intended heat stress. For this reason, this manuscript will solely focus on information derived from the corals kept at ambient temperature during TP1 when the light condition followed a typical diurnal cycle before and after sampling.

3.2 ^{15}N ammonia integration into metabolites

Tracer incorporation into the metabolome was verified using targeted LC-MS analysis. HILIC chromatography, which is ideal for resolving different polar compounds, allowed us to characterize most nitrogen-containing metabolites (Alpert 1990). High-resolution mass spectrometry not only allowed us to make more accurate metabolite annotations, but also enabled us to quantitatively evaluate isotope incorporation. When heavier isotope atoms are incorporated into metabolite structures, they result in characteristic mass shifts in the mass spectrum. Using the dipeptide arginine-glutamine (RQ), $C_{11}H_{22}N_6O_4$ ($[M+H]^+$ m/z 303.177), as an example, without labeling from a stable isotope tracer, the mass spectrum of this metabolite includes a prominent base peak corresponding to the mass-to-charge ratio (m/z) of the combination of the most abundant isotopes (Figure 2A). There is a second peak to the right of the base peak in the spectrum corresponding to the RQ dipeptide with 1 ^{13}C atom ($^{13}C_1$-RQ) due to the natural abundance of this stable isotope. Because the ^{13}C has a natural abundance of 1.01%, RQ, which has 11 C atoms, would have 10.2% being $^{13}C_1$ on average. Meanwhile, this $^{13}C_1$ peak shows the Δ mass = (m/z) 1.0034 to the base peak, which is the exact mass difference between a ^{12}C and a ^{13}C atom. When 100µM ^{15}N-NH_4Cl is introduced as the tracer, there are noticeable differences in the RQ mass spectrum. The base peak corresponding to the unlabeled RQ $^{15}N_0$-RQ is still present, and there are an additional six peaks in the spectrum (Figure 2B). Each successive peak corresponds to the mass shift due to an additionally incorporated isotopically labeled nitrogen atom, $^{15}N_1$, $^{15}N_2$, $^{15}N_3$, $^{15}N_4$, $^{15}N_5$, and $^{15}N_6$ respectively, resulting in signal observed at (m/z) = 304.175, 305.171, 306.169, 307.166, 308.163, and 309.160, respectively. Successive mass shift Δ mass = (m/z) 0.997, which corresponds to the Δ mass of ^{14}N and ^{15}N. The $^{13}C_1$-RQ peak is not observed in this spectrum because the mass resolution is insufficient to distinguish it from the $^{15}N_1$ peak (Wang et al 2021).

Targeted data analysis shows that ^{15}N-NH_4^+ is assimilated into several metabolite classes of primary and secondary metabolism. Most notably, glutamine has the highest labeled fractions (Figure 3A-F). This result is consistent with glutamine being directly synthesized by the NH_4^+ assimilating enzyme GS. Glutamate and alanine also have higher labeled fractions than the remaining amino acids, suggesting the importance of other NH_4^+ assimilating transaminases such as ALT/GOGAT and GDH (Reitzer 2004). The remaining amino acids have relatively low tracer incorporation. This precipitous decrease in detectable labeled fractions of other amino acids suggests that they have low turnover. In addition to amino acids, ^{15}N-NH_4^+ was also incorporated into purines and pyrimidine nucleotides derivatives and urea cycle metabolites (Figure 3G-K). The urea cycle metabolites ornithine and citrulline, were significantly more labeled than arginine, which is an amino acid that is also an intermediate in this pathway. The low enrichment in arginine, however, does not suggest that there is an impediment to arginine production in the pathway, Closer analysis shows that although a large fraction of arginine remains unlabeled after 18 hours incubation with ^{15}N-NH_4^+, the $^{15}N_3$ and $^{15}N_4$ labeled arginine fractions were also clearly observed. This observation confirms that there is rapid biosynthesis occurring, yet the labeled fraction is low. Labeling was also observed in some metabolic precursors and their derivatives such as NAD^+ and UDP-N-acetyl-glucosamine (Supplementary Data Table). Interestingly, as shown in Fig. 2, we also observed robust ^{15}N incorporation into dipeptides (Figure 3L-O). Our previous work demonstrated that dipeptides are a secondary metabolite class that accumulate during heat stress (Williams et al, 2021). Of the four dipeptides previously reported, all were found to be ^{15}N labeled in this study. Results were consistent among all three species of coral included in the study (*M. capitata*, *P. acuta*, and *P. compressa*) and labeled fractions were comparable among all three species tested for the vast majority of metabolites detected, therefore, the discussion of our results will focus on *M. capitata* as a representative coral species (see supplemental results for all species).

3.3 Dipeptides showed significant ^{15}N enrichment

Although the labeling fraction distribution of individual metabolites can be informative as to whether ^{15}N-NH_4^+ is incorporated into a given metabolite, it is not informative in a comparative sense of the relative isotopic incorporation between metabolites or metabolite classes. This is because different metabolites have different numbers of total nitrogen atoms that can be labeled, leading to different isotopologue distribution potentials. We, therefore, need a way to compare metabolites while accounting for individual probability of each metabolite having labeling at any one potential nitrogen atomic site. To achieve this goal, we use a metric known as enrichment, which is the average percentage of ^{15}N labeling on per N atom basis. After 18 hours of labeling with 100 µM ^{15}N-NH_4Cl, the average enrichment for primary metabolites is 5.2% ± 1.6% (mean ± SD), suggesting that there is a very low turnover rate for the pool sizes of these metabolites in scleractinian corals. In contrast to the results from other primary metabolites, dipeptides are significantly more enriched following incubation, which have an average enrichment of 16.3% ± 4.1% (mean ± SD). These results suggest there is a higher turnover of dipeptide pools.

3.4 Dipeptides are more enriched than constitutive amino acids

Dipeptides are synthesized from the condensation of two amino acids. This means that dipeptide enrichment should correspond to the free association of the constitutive amino acids needed to produce them and their respective enrichment patterns. To investigate this issue, we compared the pair-wise dipeptide enrichment to the amino acid enrichment in the same sample. Concerning Arg-Gln in *M. capitata*, whereas the enrichment of glutamine is close to the enrichment of Arg-Gln dipeptide, the enrichment of arginine is significantly lower than that of the dipeptide (Figure 4A-B). This is, again,

likely due to glutamine being a directly produced amino acid follow nitrogen assimilation via the GS enzyme. These trends are also seen in the Lys-Gln data, although the overall enrichment is lower for Lys-Gln than Arg-Gln (Figure 4C-D). Arginine is also less enriched than the dipeptide Arg-Ala, and the total enrichment is lower in this dipeptide than Arg-Gln and Lys-Gln respectively (Figure 4E). The constitutive amino acid alanine is more enriched than Arg-Ala (Figure 4F). Arg-Val is the least enriched of the previously reported dipeptides, however, arginine is still generally less enriched than the dipeptide (Figure 4G). Valine enrichment was observed to be higher in all sample pairs than the observed Arg-Val enrichment (Figure 4H). These results suggest that dipeptide enrichment deviates significantly from the enrichment of the constitutive amino acids. Similar conclusions can be reached for *P. acuta*, and *P. compressa* (Figure S3, 4A-H).

The discrepancy between the enrichment of the dipeptides and the enrichment of the constitutive amino acids can be more quantitatively assessed by calculating the theoretical enrichment of the dipeptide given the enrichment of the amino acids. Assuming the constitutive amino acids form the condensation product by free association, the enrichment of the dipeptide is the average of the amino acid enrichments weighted by their nitrogen atom numbers as described by the formula in the methods. In *M. capitata* the calculated paired sample enrichments of Arg-Gln, Lys-Gln, and Arg-Ala were all lower than the observed dipeptide measurements based on the direct metabolite measurement (Figure 5A-C). The comparison between the calculated and directly measured enrichment of Arg-Val was less robust. There are some sample pairs where the enrichment is higher in the calculated dipeptide (Figure 5D). This is likely due to the overall enrichment in this dipeptide being much lower, particularly in comparison to the remaining reported dipeptides. Calculated dipeptide enrichments values were also lower than experimentally observed enrichments in *P. acuta*, and *P. compressa*, demonstrating that this physiological phenomenon is not isolated to a single scleractinian species but is indicative of multiple coral species on the Hawaiian reefs (Figure S5A-D, S6A-C)

4 Discussion

The holobiont is a consortium that is predominantly dependent on the light-driven metabolic output of its algal symbiont community. Variations in light intensity may, therefore, result in significant biochemical differences in holobiont metabolomes. Previous work constructing photosynthesis irradiation curves of *M. capitata* samples taken from Kāneʻohe Bay and in the immediate waters around the Hawaiʻi Institute of Marine Biology show that the algal photosynthetic light saturation point is 586 ± 108 μmol quanta m^{-2} s^{-1} before calcification (growth) is negatively impacted (Langdon et al 2005). However, *M. capitata* is phenotypically plastic and able to adapt its morphology to survive within a variable range of light conditions across Kāneʻohe Bay (Padilla-Gamiño et al 2013; Innis et al 2018). The light intensity readings during our complete time course all reflect relatively low light conditions (< 300 μmol quanta m^{-2} s^{-1}). Given the wide light intensity range that *M. capitata* colonies experience in the Bay, this is not overly concerning, however, we acknowledge that for a robust analysis of how thermal stress alone impacts nitrogen metabolism that all other parameters should be as uniform as possible under a natural diurnal cycle. For this reason, we have restricted our analysis to the ambient TP1 samples that underwent a normal diurnal cycle of light availability. It is presently unclear how ubiquitously the broad light tolerance associated with *M. capitata* is exhibited by other scleractinian coral species. Therefore, elucidating how persistently low or high light levels modulate nitrogen metabolism in *M. capitata* and other species may be meritorious in its own right, as climate conditions continue to change. The experimental parameters of such studies would need to be tightly constrained.

Our work shows that ^{15}N-NH_4^+ is incorporated into a wide variety of metabolite classes. Use of a stable isotope tracer allowed us to track new metabolite production. The turnover rate of a metabolite pool is

determined by two factors, the metabolite production rate and pool size. The balance between these factors partially explains why there is low labeling in the arginine pool. Assuming a homogeneous substrate pool, the downstream product in a metabolic pathway should not have a higher stable isotope enrichment than the upstream metabolite (Buescher et al 2015; Wang et al 2020). However, in the urea cycle we observe a relatively high labeling in citrulline, followed by a low labeling in arginine, which returns to a relatively high labeling in ornithine. If the entire pool of arginine undergoes hydrolysis to produce ornithine, we should observe less labeled ornithine. Similarly, if the entire pool of citrulline goes through the urea cycle to become arginine, we should see more labeled arginine. Notably, we did observe $^{15}N_3$ and $^{15}N_4$ labeled arginine, suggesting the urea cycle is fully functional in arginine production. However, the large unlabeled fraction of arginine suggests that a large proportion of arginine is not actively turning over. In other words, there is a separate dormant pool of arginine. Dipeptide production, as evidenced by the high labeling, does not appear to be derived from the dormant arginine pool. If they were, the dipeptides would be less enriched. This work shows, however, that the arginine that is incorporated into dipeptides is mostly labeled. This would suggest that within the holobiont, there is a separate and distinct labeled pool that is used for dipeptide synthesis that exists in addition to the stable pool. Due to sample preparation limitations, the mass spectrometer does not distinguish between the dynamic pool of a metabolite in one part of the holobiont and a stable dormant pool in another. Therefore, the measurement is a reflection of the entire metabolite pool irrespective of subcellular compartmentalization (Buescher et al 2015). A large dormant pool of arginine reduces total enrichment, despite active synthesis of arginine in nitrogen assimilation.

We postulate that dipeptides are rapidly synthesized from condensation reactions of free amino acids by specific ligases. Such reactions and dipeptide products have been studied extensively in mammals. For instance, carnosine, which is a dipeptide of β-alanine and histidine, is synthesized by carnosine synthase, and is found primarily in skeletal muscle and neurological tissues where its accumulation is linked to quenching reactive oxidative stress and neutralizing lactic acid build-up (Aldini et al 2005; Bonfanti et al 1999). Kyotorphin, which is a dipeptide of tyrosine and arginine and is produced by kyotorphin synthase, is a neuroactive analgesic metabolite (Takagi et al 1979; Ueda et al 1987). We believe such ligases are responsible for the production of stress related dipeptides in corals. The alternative hypothesis would be that these dipeptides are proteolytic products. However, if proteins were the precursors for the dipeptide production observed in this study, it would follow the same tenants of tracer studies attributed to the metabolite pools, which is to say that the protein pool would have to be labeled in excess of the dipeptide pool, which is highly unlikely given that labeling of the protein pool would be slower than the labeling of the metabolite pool. Nonetheless, to say with absolute certainty that the rapid turnover of the dipeptide pool observed in this work is not due to proteolysis, an analogous sample set prepared for proteomics must be analyzed, which is also an area well suited for the LC-MS platform. We, therefore, focused on considering the results of this work from the perspective that dipeptide synthesis is the result of amino acids conjoining, meaning that the dipeptide enrichment should be explained from the observed amino acid enrichment. We investigated this by examining the enrichment. To understand if dipeptide production is directly attributed to amino acid production, the pair-wise enrichment of dipeptides was compared to the enrichment in the constitutive amino acids that would be used to make the dipeptide. Here we concluded that the dipeptides are more enriched than can be explained by the random association of amino acids and, therefore, there must be a distinct biosynthetic mechanism for their production.

If the enrichment of dipeptides cannot be attributed to proteolysis or solely to amino acid enrichment, then another mechanism must explain the observed rapid synthesis of holobiont dipeptides. Our results implicate sequestration of nitrogen assimilation in corals. Although dipeptides and individual amino acids are both reliant on nitrogen sources for their biosynthesis, these metabolite pools are distinct

within holobiont compartments (Figure 6). The data also suggest that there is rapid and concerted dipeptide biosynthesis of secondary metabolites shortly after the assimilation of free nitrogen into the holobiont. We postulate that, although both the coral animal host and the Symbiodiniaceae have the enzymatic machinery to assimilate nitrogen into the holobiont, the bulk of this activity occurs within Symbiodiniaceae and is powered by light energy. The Symbiodiniaceae is likely also where amino acids are rapidly incorporated into a dipeptide pool before they are shunted to the coral animal host with the remaining photosynthate products. Dipeptides have been implicated in the oxidative stress response in murine models (Nagasawa et al 2001; Rezzani et al 2019). It has been proposed that nitrogen restriction allows the coral host to control the algal symbiont growth and proliferation (Cui et al 2022; Pupier et al 2021). It is possible that rapid synthesis of amino acids into dipeptides allows Symbiodiniaceae to diminish bioavailability of nitrogen to reduce the potential influence of host nitrogen mediated control. This may also help explain the confounding phenomenon of differences in bleaching susceptibility among Symbiodiniaceae clades (González-Pech et al 2021; Matsuda et al 2021; Silverstein et al 2015). More resilient symbiont clades may have an increased ability to mediate host nitrogen restriction via nitrogen sequestration into dipeptides. Investigating the biological significance of rapid dipeptide production, the broader role dipeptides play with respect to bleaching, and how nitrogen metabolism is altered under stress conditions are areas of ongoing research. In future studies, we will extend our use of stable isotope tracing to investigate how environmental stressors, such as heat and high light conditions, alter homeostatic holobiont nitrogen metabolism by using more controlled bleaching experiments. This will be coupled to matrix-assisted laser desorption ionization (MALDI) imaging mass spectrometry to determine the spatial distribution of metabolites that incorporate nitrogen within the holobiont to further understand nitrogen cycling and holobiont metabolite exchange (Wang et al 2022). Greater understanding of how the microbial community and the host adapt their nitrogen assimilation mechanisms in response to stressors may be a crucial component of improving our understanding of overall reef resilience in the field.

5 Data Availability Statement

The metabolomics datasets presented in this study can be found in the MassIVE database under project number MSV000090231. The original contributions presented in the study are included in the manuscript and/or Supplementary Material. Additional inquiries can be directed to the corresponding author.

6 Author Contributions

ENC, XS, and DB conceived the study. ENC and XS designed the fieldwork experiment strategy. HMP provided coral tissues for analysis, ENC, AH, HMP, and CD performed the fieldwork experiments. ENC analyzed the samples and performed the bioinformatics. ENC, XS, DB, and AH contributed to data interpretation. ENC wrote the original draft of the manuscript. XS, DB, HMP, AH, and CD revised the original draft. All authors have read and approve of the submitted version of the manuscript.

7 Funding

The metabolomics analysis was performed at the Rutgers Cancer Institute of New Jersey Metabolomics Shared Resource and supported, in part, by funding from NCI-CCSG, P30CA072720-5923. This work was supported by a grant from the Catalyst Science Fund-Revive and Restore award to DB and XS, in addition to National Science Foundation award 1756623 to HMP. DB was also supported by NSF grant NSF-OCE 1756616 and a NIFA-USDA Hatch grant (NJ01180).

8 Conflict of Interest

The authors declare that the research was conducted in the absence of any commercial or financial relationships that could be construed as a potential conflict of interest.

9 Publisher's Note

All claims expressed in this article are solely those of the authors and do not necessarily represent those of their affiliated organizations, or those of the publisher, the editors and the reviewers. Any product that may be evaluated in this article, or claim that may be made by its manufacturer, is not guaranteed or endorsed by the publisher.

10 Acknowledgments

We acknowledge the Hawai'i Institute of Marine Biology Coral Resilience Lab, Rob Toonin, and Christopher Suchoki for their resources to support this work, Jill Ashley for metadata analysis script assistance, and Dr. Yujue Wang for his valuable comments and suggestions.

11 Supplementary Material

The Supplementary Material for this article can be found online at:

12 References

Aldini G., Facino R.M., Beretta G., Carini M. (2005). Carnosine and related dipeptides as quenchers of reactive carbonyl species: From structural studies to therapeutic perspectives. *BioFactors*. 24, 77-87.

Alpert A.J. (1990). Hydrophilic-interaction chromatography for the separation of peptides, nucleic acids and other polar compounds. *Journal of Chromatography*. 19, 177-196. doi: 10.1016/s0021-9673(00)96972-3

Badger, M., & Price, G. (1992). The CO2 concentrating mechanism in cyanobacteria and microalgae. *Physiologia Plantarum - Physiol Plant*. 84, 606-615. doi: 10.1034/j.1399-3054.1992.840416.x

Bahr, K. D., Jokiel, P. L., & Rodgers, K. S. (2015). The 2014 coral bleaching and freshwater flood events in Kāne'ohe Bay, Hawai'i. *PeerJ*, 3, e1136. doi: 10.7717/peerj.1136

Benavides M., Bednarz V. N., Ferrier-Pagès C. (2017). Diazotrophs: overlooked key players within the coral symbiosis and tropical reef ecosystems? *Front. Mar. Sci.* doi: 10.3389/fmars.2017.00010

Bonfanti L., Peretto P., De Marchis S., Fasolo A. (1999). Carnosine-related dipeptides in the mammalian brain. *Progress in Neurobiology*. 59, 333-353. doi: 10.1016/S0301-0082(99)00010-6

Bourne D.G., Morrow K.M., Webster N.S. (2016). Insights into the coral microbiome: Underpinning the health and resilience of reef ecosystems. *Annu. Rev. Microbiol*. 70, 317–340. doi: 10.1146/annurev-micro-102215-095440

Buescher J.M., Antoniewicz M.R., Boros L.G., Burgess S.C., Brunengraber H., Clish C.B., DeBerardinis R.J., Feron O., Frezza C., Ghesquiere B., Gottlieb E., Hiller K., Jones R.G., Kamphorst J.J., Kibbey R.G., Kimmelman A.C., Locasale J.W., Lunt S.Y., Maddocks O.D., Malloy C., Metallo C.M., Meuillet E.J., Munger J., Nöh K., Rabinowitz J.D., Ralser M., Sauer U., Stephanopoulos G., St-Pierre J., Tennant D.A., Wittmann C., Vander Heiden M.G., Vazquez A., Vousden K., Young J.D.,

Zamboni N., Fendt S.M. (2015) A roadmap for interpreting (13)C metabolite labeling patterns from cells. *Curr Opin Biotechnol*. 34, 189-201. doi: 10.1016/j.copbio.2015.02.003.

Burriesci, M.S., Kaab, T.K., Pringle, J.R. (2012). Evidence that glucose is the major transferred metabolite in dinoflagellate-cnidarian symbiosis. *J Exp Biol*. 215, 3467-3477. doi: 10.1242/jeb.070946

Cleves, P.A., Krediet, C.J., Lehnert, E.M., Onishi, M., Pringle, J.R. (2020). Insights into coral bleaching under heat stress from analysis of gene expression in a sea anemone model system. *PNAS*. 117, 28906-28917. doi: 10.1073/pnas.2015737117

Cui G., Liew Y.J., Konciute M.K. Zhan Y., Hung S.H., Thistle J., Gastoldi L., Schmidt-Roach S., Dekker J., Aranda M. (2022). Nutritional control regulates symbiont proliferation and life history in coral-dinoflagellate symbiosis. *BMC Biol*. doi: 10.1186/s12915-022-01306-2

Cunning R., Baker A. (2013). Excess algal symbionts increase the susceptibility of reef corals to bleaching. Nature Climate Change. 2013; 3. 259-262, 10.1038/nclimate1711

Falkowski P.G., Dubinsky Z., Muscatine L., McCloskey L. (1993). Population Control in Symbiotic Corals: Ammonium ions and organic materials maintain the density of zooxanthellae. *BioScience*. 43, 606–611. doi: 10.2307/1312147

Forsman Z., Kimokeo B., Bird C., Hunter C., & Toonen R. (2012). Coral farming: Effects of light, water motion and artificial foods. *Journal of the Marine Biological Association of the United Kingdom, 92*, 721-729. doi:10.1017/S0025315411001500

Furla P., Allemand D., Shick J.M., Ferrier-Pagès C., Richier S., Plantivaux R.S., Merle P.L., Tambutté S. (2005). The Symbiotic Anthozoan: A Physiological Chimera between Alga and Animal, *Integrative and Comparative Biology*. 45, 595–604 doi: 10.1093/icb/45.4.595

Furla P., Galgani I., Durand I. *et al*. (2000). Sources and mechanisms of inorganic carbon transport for coral calcification and photosynthesis. *J Exp Biol*. 203, 3445–3457. doi: 10.1242/jeb.203.22.3445

González-Pech R.A., Stephens T.G., Chen, Y. Mohamed A.R., Cheng Y., Shah S., Dougan K.E., Fortuin M.D.A., Lagorce R., Burt D.W., Bhattacharya D., Ragan M.A., Chan C.X. (2021). Comparison of 15 dinoflagellate genomes reveals extensive sequence and structural divergence in family Symbiodiniaceae and genus *Symbiodinium*. *BMC Biol*. doi: 10.1186/s12915-021-00994-6

Grover R., Maguer J. F., Allemand D., Ferrier-Pagès C. (2006). Urea uptake by the Scleractinian coral *Stylophora pistillata*. *J. Exp. Mar. Bio. Ecol.* 332, 216–225. doi: 10.1016/j.jembe.2005.11.020

Grover R., Maguer J. F., Allemand D., Ferrier-Pagès C. (2008). Uptake of dissolved free amino acids by the Scleractinian coral *Stylophora pistillata*. *J. Exp. Biol.* 211, 860–865. doi: 10.1242/jeb.012807

Grover R., Maguer J. F., Reynaud-Vaganay S., Ferrier-Pagès C. (2002). Uptake of ammonium by the Scleractinian coral *Stylophora pistillata*: effect of feeding, light, and ammonium concentrations. *Limnol. Oceanogr.* 47, 782–790. doi: 10.4319/lo.2002.47.3.0782

Grover R., Maguer J.-F., Allemand D., Ferrier-Pagès C. (2003). Nitrate uptake in the Scleractinian coral *Stylophora pistillata*. *Limnol. Oceanogr.* 48, 2266–2274. doi: 10.4319/lo.2003.48.6.2266

509 Hillyer K.E., Dias D., Lutz A., Roessner U., Davy S. (2018). ^{13}C metabolomics reveals widespread
510 change in carbon fate during coral bleaching. *Metabolomics*. 14**,** 12. doi: 10.1007/s11306-017-1306-8

511 Hoegh-Guldberg O., Pendleton L., Kaup A. (2019). People and the changing nature of coral reefs.
512 *Regional Studies in Marine Science*. https://doi.org/10.1016/j.rsma.2019.100699.

513 Innis T., Cunning R., Ritson-Williams R., Wall C.B., Gates R.D. (2018) Coral color and depth drive
514 symbiosis ecology of *Montipora capitata* in Kāneʻohe Bay, Oʻahu, Hawaiʻi. *Coral Reefs*. 37, 423-430.
515 doi: 10.1007/s00338-018-1667-0

516 Jang C, Chen L, Rabinowitz JD. (2018). Metabolomics and isotope tracing. *Cell*. 3, 822-837. doi:
517 10.1016/j.cell.2018.03.055

518 LaJeunesse T. C., Parkinson J. E., Gabrielson P. W., Jeong H. J., Reimer J. D., Voolstra C. R., Santos
519 S.R. (2018). Systematic revision of Symbiodiniaceae highlights the antiquity and diversity of coral
520 endosymbionts. *Curr. Biol.* 28 2570–2580. 10.1016/j.cub.2018.07.008

521 Langdon C. and Atkinson M.J. (2005). Effect of elevated pCO2 on photosynthesis and calcification of
522 corals and interactions with seasonal change in temperature/irradiance and nutrient enrichment.
523 *Journal of Geophysical Research: Oceans*. doi:10.1029/2004JC002576

524 Li, T., Chen, X., & Lin., S. (2021). Physiological and transcriptomic responses to N-deficiency and
525 ammonium: Nitrate shift in *Fugacium kawagutii* (Symbiodiniaceae). *Science of the Total Environment*.
526 doi: 10.1016/j.scitotenv.2020.141906

527 Loya Y., Sakai K., Yamazato K., Nakano Y., Sambali H., van Worsik R. (2001). Coral bleaching: the
528 winners and the losers. *Ecology Letters*. 4, 122-131. doi: 10.1046/j.1461-0248.2001.00203.x

529 Mackay G. M., Zheng L., van den Broek N.J.F., Gottlieb E. (2015). Chapter Five - Analysis of Cell
530 Metabolism Using LC-MS and Isotope Tracers. *Methods in Enzymology*. 561, 171-196. doi:
531 10.1016/bs.mie.2015.05.016

532 Matsuda, S.B., Chakravarti, L.J., Cunning, R., Huffmyer, A., Nelson, C.E., Gates, R.D., van Oppen,
533 M.J.H. (2021). Temperature-mediated acquisition of rare heterologous symbionts promotes survival of
534 coral larvae under ocean warming. *Global Change Biology*. doi: 10.1111/gcb.16057

535 Mcclanahan T., Polunin N., Done T. (2002). Ecological States and the Resilience of Coral Reefs.
536 *Conservation Ecology*. doi: 10.5751/ES-00461-060218

537 Melamud E., Vastag L., Rabinowitz J.D. (2010). Metabolomic analysis and visualization engine for
538 LC-MS data. *Anal. Chem*. 82, 9818–9826 doi: 10.1021/ac1021166

539 Muscatine L., Masuda H., Burnap R. (1979). Ammonium uptake by symbiotic and aposymbiotic reef
540 corals. *Bull. Mar. Sci.* 29 572–575.

541 Nagasawa T., Yonekura T., Nishizawa N., Kitts D.D. (2001). In vitro and in vivo inhibition of muscle
542 lipid and protein oxidation by carnosine. *Mol. Cell. Biochem.* 225, 29–34.
543 doi: 10.1023/A:1012256521840

Nielsen D.A., Petrou K., Gates R.D. (2018). Coral bleaching from a single cell perspective. *ISME J*. 12, 1558–1567. doi: 10.1038/s41396-018-0080-6

Padilla-Gamiño J.L., Bidigare R.R., Barshis D.J., Alamaru A., Hédouin L., Hernábdez-Pech X., Kandel F., Soon S.L., Roth M.S., Rodrigues L.J., Grottoli A.G., Portocarrero C., Wagenhauser S.A., Buttler F., Gates R.D. (2013). Are all eggs created equal? A case study from the Hawaiian reef-building coral *Montipora capitata*. *Coral Reefs*. 32, 137–152. doi: 10.1007/s00338-012-0957-1

Pernice M., Meibom A., Van Den Heuvel A., Kopp C., Domart-Coulon I., Hoegh-Guldberg O., Dove S. (2012). A single-cell view of ammonium assimilation in coral–dinoflagellate symbiosis. *ISME J*. 6, 1314–1324. doi: 10.1038/ismej.2011.196

Pogoreutz, C., Rädecker, N., Cardenas, A., Gärdes, A., Voolstra, C. R., & Wild, C. (2017). Sugar enrichment provides evidence for a role of nitrogen fixation in coral bleaching. *Global Change Biology*, *23*(9), 3838-3848. doi: 10.1111/gcb.13695

Pupier C.A., Grover R., Fine M., Rottier C., van de Water J.A.J.M., Ferrier-Pagès C. (2021). Dissolved Nitrogen Acquisition in the Symbioses of Soft and Hard Corals With Symbiodiniaceae: A Key to Understanding Their Different Nutritional Strategies? *Front Microbiol*. doi: 10.3389/fmicb.2021.657759

Rädecker N., Pogoreutz C., Gegner H.M., Cardenas A., Roth F., Bougoure J., Guagliardo P., Wild., Pernice M., Raina JB., Meibom A., Voolstra C. (2020). Heat stress destabilizes symbiotic nutrient cycling in corals. *PNAS*. 118, 1-11. doi: 10.1073/pnas.2022653118

Rädecker N., Pogoreutz C., Voolstra C., Wiedenmann J., Wild C. (2015). Nitrogen cycling in corals: the key to understanding holobiont functioning. *Trends in Microbiology*. 23, 490-497. doi: 10.1016/j.tim.2015.03.008

Reitzer L. (2004). Biosynthesis of glutamate, aspartate, asparagine, L-alanine, and D-alanine. *American Society for Microbiology EcoSal Plus*. doi: 10.1128/ecosalplus.3.6.1.3

Rezzani R., Favero G., Ferroni M., Lonati C., Moghadasian M.H. (2019). A carnosine analog with therapeutic potentials in the treatment of disorders related to oxidative stress. *PLoS ONE*. doi: 10.1371/journal.pone.0215170

Roberts, J.M., Fixter, L.M. & Davies, P.S. (2001). Ammonium metabolism in the symbiotic sea anemone *Anemonia viridis*. *Hydrobiologia*. 461, 25–35. doi: 10.1023/A:1012752828587

Roth, M. (2013). The engine of the reef: photobiology of the coral–algal symbiosis. *Frontiers in Microbiology*. doi: 10.3389/fmicb.2014.00422

Silverstein, R.N., Cunning, R., Baker, A. (2015). Change in algal symbiont communities after bleaching, not prior heat exposure, increases heat tolerance of reef corals. *Global Change Biology*, 21, 236–249. doi: 10.1111/gcb.12706

Sogin E., Putnam H., Anderson P., Gates R. (2016). Metabolomic signatures of increases in temperature and ocean acidification from the reef-building coral, *Pocillopora damicornis*. *Metabolomics*. doi: 10.1007/s11306-016-0987-8

Su X., Lu W., Rabinowitz J.D. (2017). Metabolite spectral accuracy on orbitraps. *Analytical Chemistry*. *89*, 5940-5948. doi: 10.1021/acs.analchem.7b00396

Takagi H., Shiomi H., Ueda H., Amano H. (1979). A novel analgesic dipeptide from bovine brain is a possible Met-enkephalin releaser. *Nature*. 282, 410-412. doi: 10.1038/282410a0

Tivey T.R., Parkinson J.E., Weis V.M. (2020). Host and symbiont cell cycle coordination is mediated by symbiotic state, nutrition, and partner identity in a model cnidarian dinoflagellate symbiosis. *American Society for Microbiology MBio*. doi: 10.1128/mBio.02626-19

Ueda H., Yoshihara Y., Fukushima N., Shiomo H., Nakamura A., Takagi H. (1987). Kyotorphin (tyrosine-arginine) synthetase in rat brain synaptosomes. *Journal of Biological Chemistry*. 262, 8165-8173.

Wang L., Xing X., Zeng X., Jackson R., TeSlaa T., Al-Dalahmah O., Samarah L., Goodwin K., Yang L., McReynolds M., Li., Wolff., Rabinowitz., J.D., Davidson S.M. (2022). Spatially resolved isotope tracing reveals tissue metabolic activity. *Nature Methods*. 19, 223–230 doi: 10.1038/s41592-021-01378-y

Wang Y., Parsons L.R., Su X. (2021). AccuCor2: isotope natural abundance correction for dual-isotope tracer experiments. *Laboratory Investigation*. 101, 1403–1410. doi: 10.1038/s41374-021-00631-4

Wang Y., Wondisford F.E., Song C., Zhang T., Su X. (2020). Metabolic flux analysis-linking isotope and metabolic fluxes. *Metabolites*. doi: 10.3390/metabo10110447

Whitney S.M. and Yellowlees D. (1995). Preliminary investigations into the structure and activity of ribulose bisphosphate carboxylase from two photosynthetic dinoflagellates. *Journal of Phycology*. 31, 138-146. doi: 10.1111/j.0022-3646.1995.00138.x

Whitney S.M., Shaw D.C., Yellowlees D. (1995). Evidence that some dinoflagellates contain a ribulose-1,5-bisphosphate carboxylase / oxygenase related to that of the α-proteobacteria. *Proc. R. Soc. Lond. B*. 259, 271–275. doi: 10.1098/rspb.1995.0040

Wilkinson D.J. (2016) Historical and contemporary stable isotope tracer approaches to studying mammalian protein metabolism. *Mass Spectrometry Reviews*. 37, 57-80. doi: 10.1002/mas.21507

Williams A., Chiles E.N., Conetta D., Pathmanathan J.S., Cleves P.A., Putnam H.M., Su X., Bhattacharya D. (2021). Metabolomic shifts associated with heat stress in coral holobionts. *Science Advances*. 7. doi: 10.1126/sciadv.abd4210

Zamboni N., Saghatelian A., Patti G.J. (2015) Defining the metabolome: size, flux, and regulation. *Molecular Cell*. 58, 699-706. doi: 10.1016/j.molcel.2015.04.021

13 Figure Captions

Figure 1. Culture and ^{15}N labeling of Hawaiian stony corals.

(**A** to **C**) Images of *Montipora capitata*, *Pocillopora acuta*, and *Porites compressa* from Kāneʻohe Bay, Oʻahu. Photo credit: D. Bhattacharya. (**D**) Schematic of the experimental design depicting an isotopic incubation of stony corals in filtered seawater supplemented with 100 μM ^{15}N-NH$_4$Cl. (**E**) Pathway

showing the incorporation of ammonia as a nitrogen source into corals. Nitrogen is assimilated from ammonia to α-ketoglutarate to produce glutamate by the enzyme glutamate dehydrogenase (GDH). A further nitrogen atom is incorporated through amination onto glutamate to produce glutamine with the enzymes glutamine synthetase (GS) and/or glutamine oxoglutarate aminotransferase (GOGAT). Glutamate is used a precursor for the production of many additional amino acids including lysine (Lys), valine (Val), alanine (Ala), and arginine (Arg) through various steps. Glutamate can also be shunted to urea cycle in which ornithine (Orn) and citrulline (Cit) are made (**F**) Tank temperature trace for *M. capitata*, *P. acuta*, and *P. compressa* samples kept during the experiment conducted at the Hawai'i Institute of Marine Biology. (**G**) Tank light trace for *M. capitata*, *P. acuta*, and *P. compressa* samples kept during the experiment conducted at the Hawai'i Institute of Marine Biology.

Figure 2. Spectra comparison of non-labeled ^{14}N and labeled ^{15}N arginine-glutamine dipeptide.

(**A**) Mass spectral pattern for the dipeptide arginine-glutamine (RQ $C_{11}H_{22}N_6O_4$) under ^{14}N conditions. There is a base peak in the spectrum that corresponds to the mass of the RQ dipeptide under positive ionization polarity, m/z = 303.177. A secondary minor peak in the spectra that corresponds to the ^{13}C natural abundance peak, as determined by the Δ mass = 1.0034 to the base peak. (**B**) Mass spectral pattern for the dipeptide arginine-glutamine (RQ) under stable isotope ^{15}N NH_4Cl incubated conditions. There is a base peak in the spectra that corresponds to the mass of the RQ dipeptide under positive ionization polarity, m/z = 303.177. There are six successive peaks in the spectra caused by the mass shifts due to each successive nitrogen atom, as determined by the Δ mass = 0.997 to the base peak and each successive peak.

Figure 3. ^{15}N-NH_4^+ incorporation in several metabolite classes.

(**A** to **F**) Labeled fraction stacked bar plots for several amino acid class metabolites. (**G** to **I**) Labeled fraction stacked bar plots for several purine and pyrimidine class metabolites. (**J** to **K**) Labeled fraction stacked bar plots for several urea cycle class metabolites. (**L** to **O**) Labeled fraction stacked bar plots for several dipeptide class metabolites. Plots depict the labeling pattern of three ambient temperature biological replicate tanks for *M. capitata*, *P. acuta*, and *P.compressa* respectively. The fraction number indicates the number of ^{15}N being incorporated. Error bars reflect technical replicate of n=3 for each individual tank sampling.

Figure 4. Comparison of dipeptide and constitutive amino acid enrichment in *M. capitata*.

(**A** to **B**) Comparison of the enrichment arginine and glutamine to the enrichment of the dipeptide arginine-glutamine. (**C** to **D**) Comparison of the enrichment lysine and glutamine to the enrichment of the dipeptide lysine-glutamine. (**E** to **F**) Comparison of the enrichment arginine and alanine to the enrichment of the dipeptide arginine-alanine. (**G** to **H**) Comparison of the enrichment arginine and valine to the enrichment of the dipeptide arginine-valine. Asterisks denote significance at *P <0.05, **P <0.01, ***P <0.001.

Figure 5. Comparison of calculated dipeptide and experimentally observed dipeptide enrichment in *M. capitata*.

(**A**) Comparison of the calculated enrichment of arginine-glutamine based on the enrichments of the respective constitutive amino acids to the experimentally measured enrichment of arginine-glutamine pool directly. (**B**) Comparison of the calculated enrichment of lysine-glutamine based on the enrichments of the respective constitutive amino acids to the experimentally measured enrichment of lysine-glutamine pool directly. (**C**) Comparison of the calculated enrichment of arginine-alanine based

on the enrichments of the respective constitutive amino acids to the experimentally measured enrichment of arginine-alanine pool directly. (**D**) Comparison of the calculated enrichment of arginine-valine based on the enrichments of the respective constitutive amino acids to the experimentally measured enrichment of arginine-valine pool directly. Asterisks denote significance at *P <0.05, **P <0.01, ***P <0.001.

Figure 6. Proposed schematic of the mechanism for nitrogen assimilation in scleractinian corals.

The schematic proposes the ways major nitrogen sources are incorporated in the coral holobiont. Glutamate dehydrogenase (GDH), glutamine synthetase (GS), and glutamine oxoglutarate aminotransferase (GOGAT) enzymes needed for nitrogen incorporation are found in both the host coral animal and the Symbiodiniaceae, but are likely less active in the host organism than in the Symbiodiniaceae. These enzymes produce glutamine and glutamate as precursors for the production of the remaining downstream amino acids. There is a rapid and dynamic incorporation of amino acids into dipeptide products immediately after production before they are assimilated into the more stable amino acid pools.

Figure 1.TIF

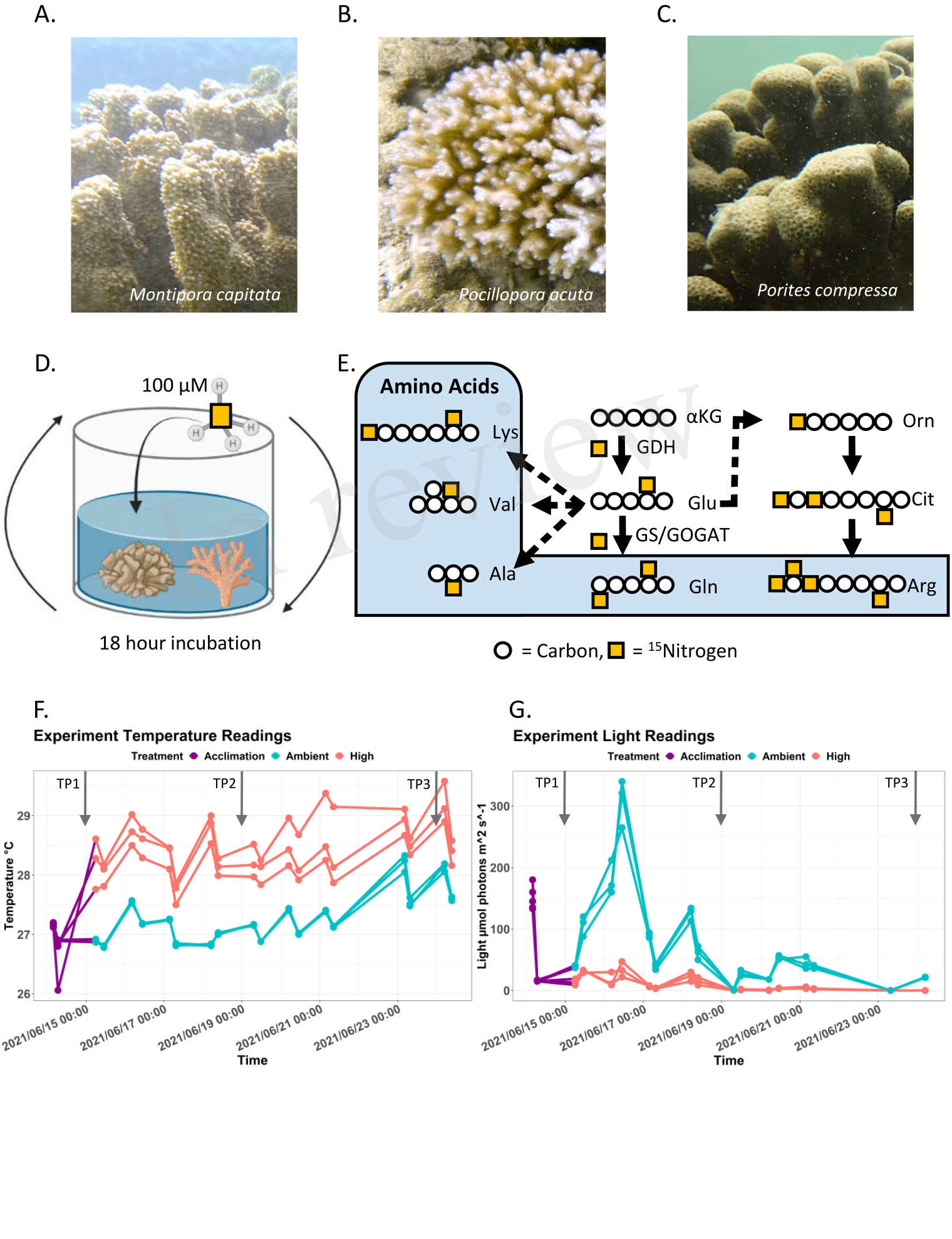
A.
Montipora capitata
B.
Pocillopora acuta
C.
Porites compressa
D.
100 µM
18 hour incubation
E.
Amino Acids
Lys
Val
Ala
αKG
GDH
Glu
GS/GOGAT
Gln
Orn
Cit
Arg
= Carbon, = 15Nitrogen
F.
Experiment Temperature Readings
Treatment Acclimation Ambient High
TP1
TP2
TP3
Temperature °C
29
28
27
26
2021/06/15 00:00
2021/06/17 00:00
2021/06/19 00:00
2021/06/21 00:00
2021/06/23 00:00
Time
G.
Experiment Light Readings
Treatment Acclimation Ambient High
TP1
TP2
TP3
Light µmol photons m^2 s^-1
300
200
100
0
2021/06/15 00:00
2021/06/17 00:00
2021/06/19 00:00
2021/06/21 00:00
2021/06/23 00:00
Time

Figure 2.TIF

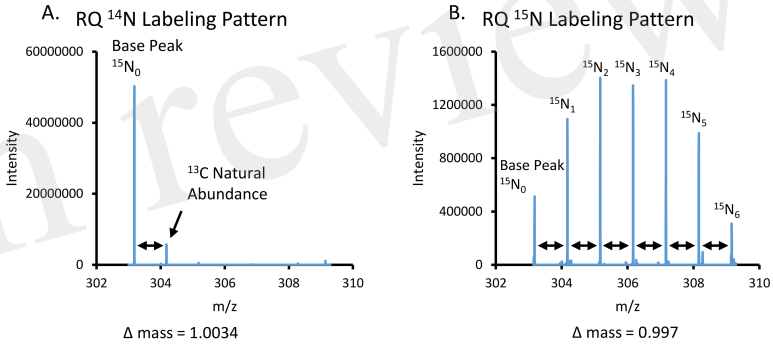

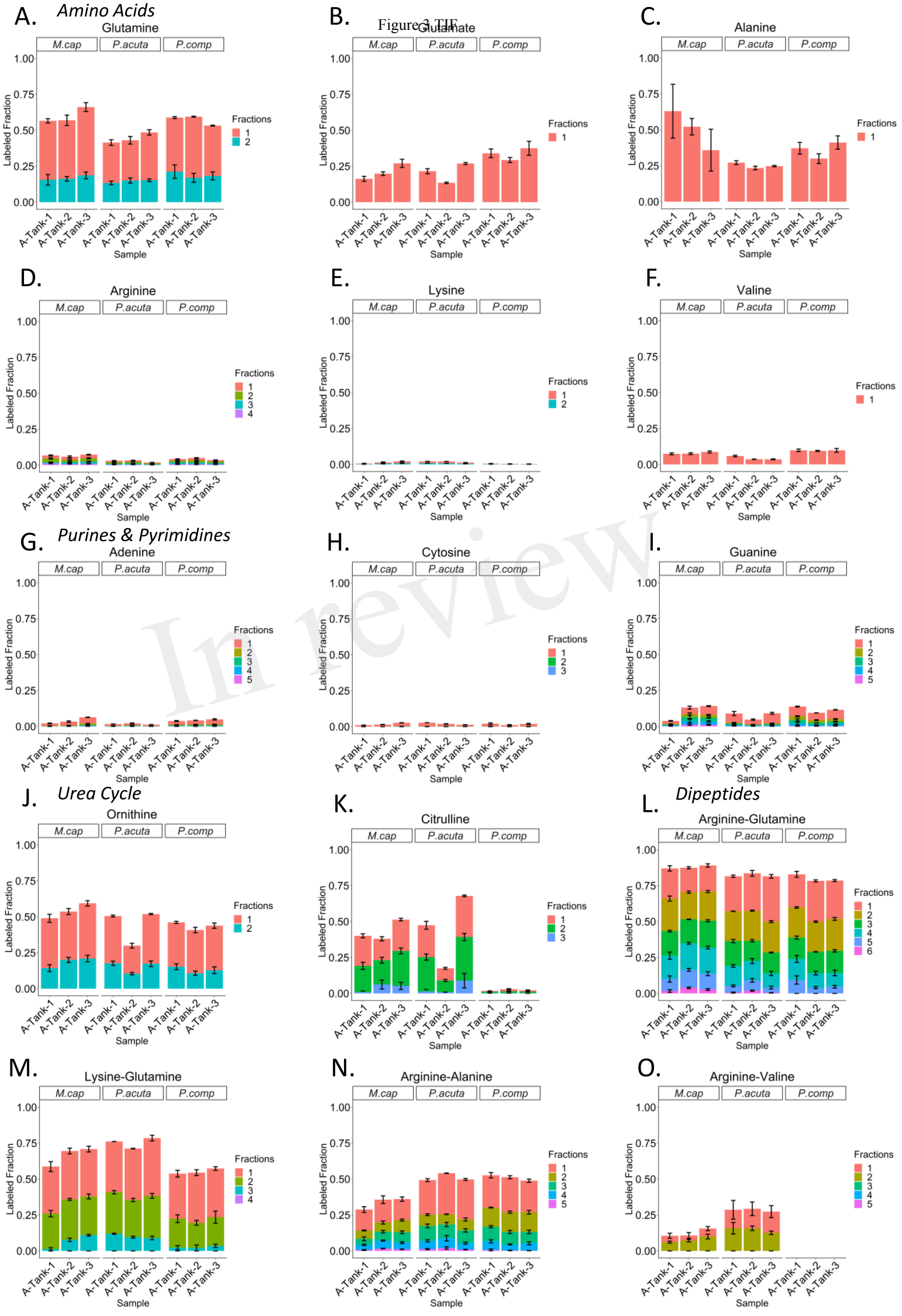
A.
Amino Acids
Glutamine
B.
Glutamate
C.
Alanine
D.
Arginine
E.
Lysine
F.
Valine
G.
Purines & Pyrimidines
Adenine
H.
Cytosine
I.
Guanine
J.
Urea Cycle
Ornithine
K.
Citrulline
L.
Dipeptides
Arginine-Glutamine
M.
Lysine-Glutamine
N.
Arginine-Alanine
O.
Arginine-Valine
M.cap
P.acuta
P.comp
Labeled Fraction
Fractions
Sample
A-Tank-1
A-Tank-2
A-Tank-3

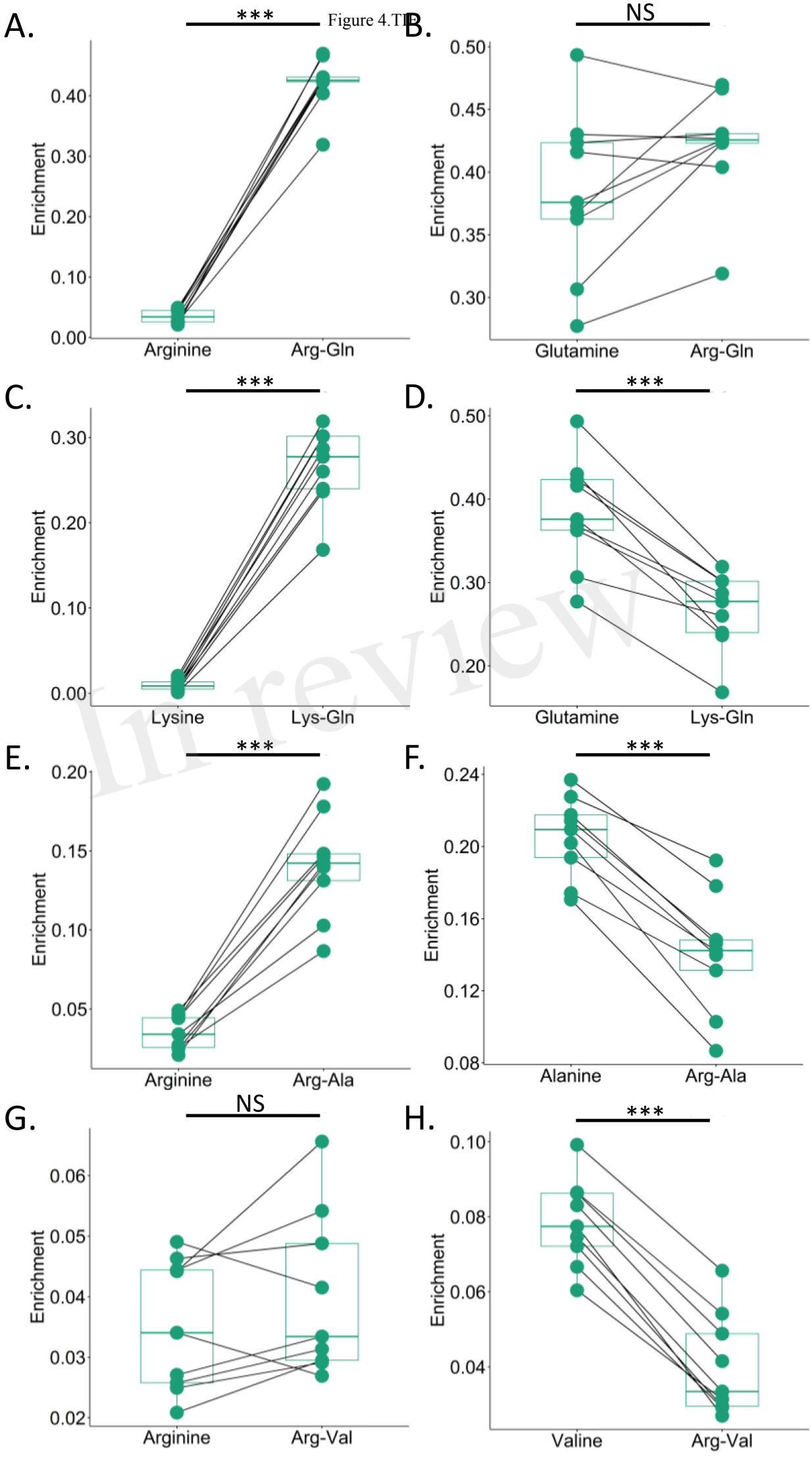
A.
***
Enrichment
0.00
0.10
0.20
0.30
0.40
Arginine
Arg-Gln
B.
NS
Enrichment
0.30
0.35
0.40
0.45
0.50
Glutamine
Arg-Gln
C.
***
Enrichment
0.00
0.10
0.20
0.30
Lysine
Lys-Gln
D.
***
Enrichment
0.20
0.30
0.40
0.50
Glutamine
Lys-Gln
E.
***
Enrichment
0.05
0.10
0.15
0.20
Arginine
Arg-Ala
F.
***
Enrichment
0.08
0.12
0.16
0.20
0.24
Alanine
Arg-Ala
G.
NS
Enrichment
0.02
0.03
0.04
0.05
0.06
Arginine
Arg-Val
H.
***
Enrichment
0.04
0.06
0.08
0.10
Valine
Arg-Val

Figure 5.TIF

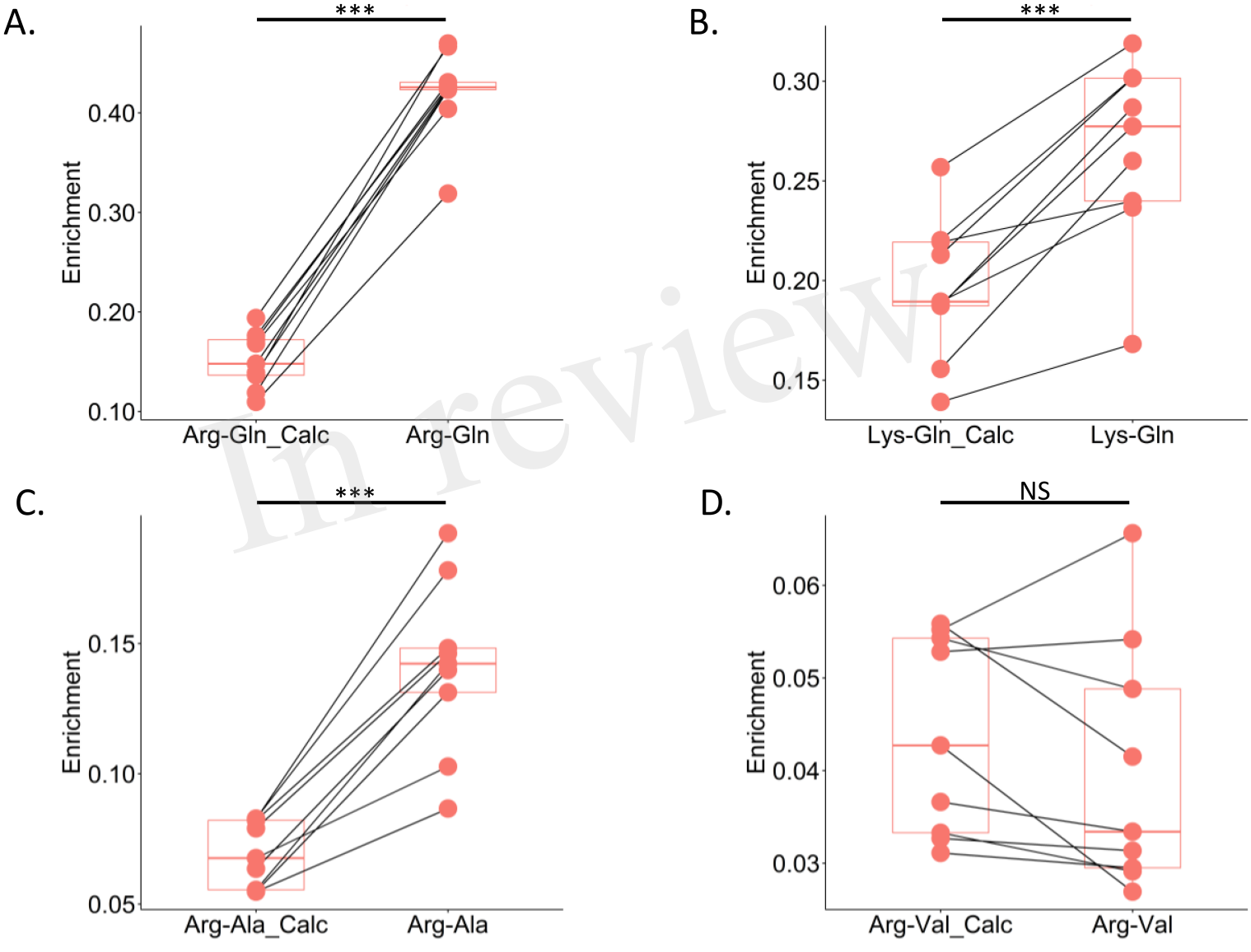

Figure 6.TIF

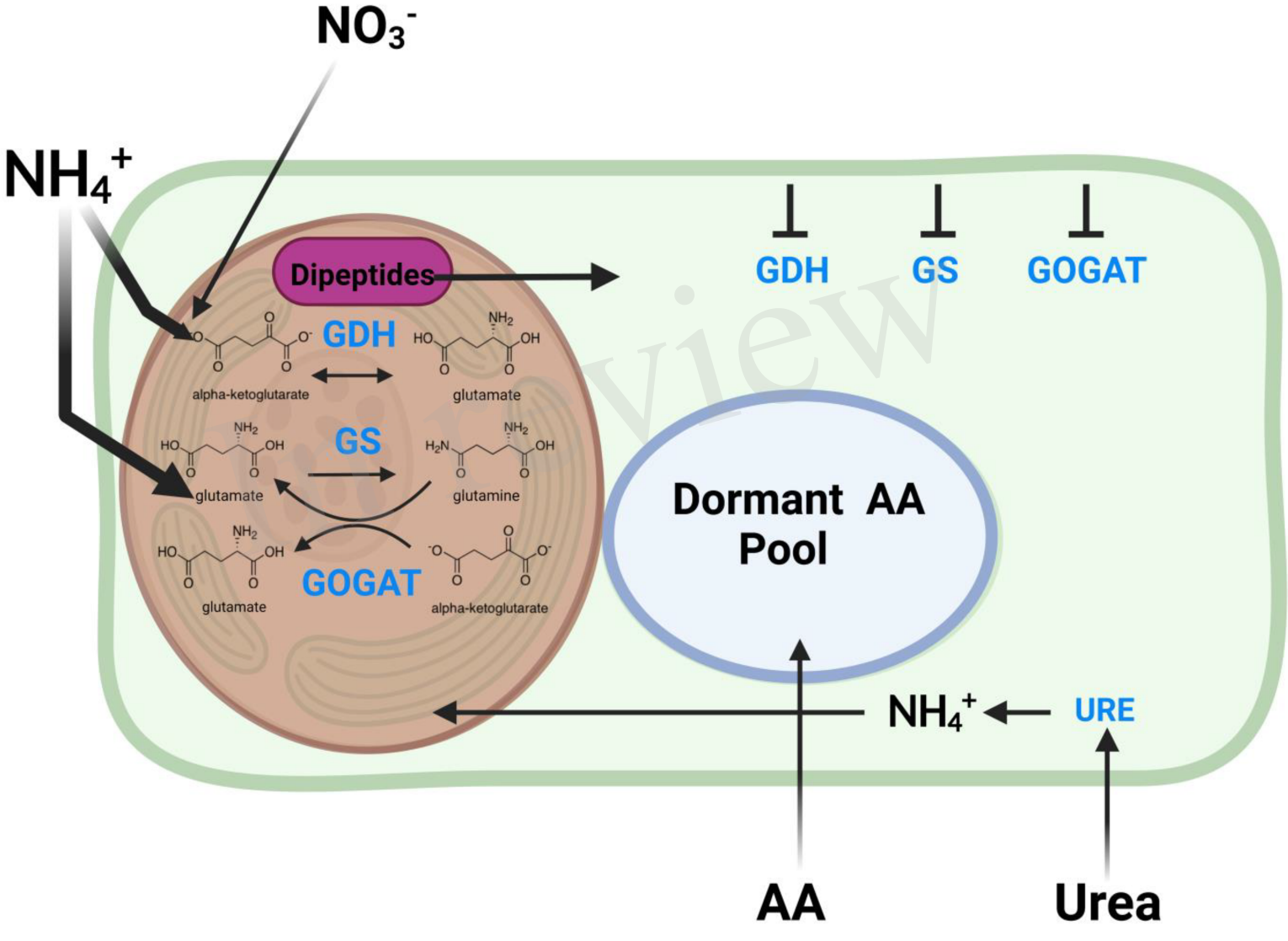
NO3-
NH4+
Dipeptides
GDH
GS
GOGAT
alpha-ketoglutarate
glutamate
glutamate
glutamine
glutamate
alpha-ketoglutarate
Dormant AA Pool
NH4+
URE
AA
Urea